Available online at www.sciencedirect.com
SCIENCE DIRECT®
International Journal of Heat and Mass Transfer 49 (2006) 144–153
International Journal of HEAT and MASS TRANSFER
www.elsevier.com/locate/ijhmt

Conjugated shear stress and Prandtl number effects on reflux condensation heat transfer inside a vertical tube

U. Gross *, Ch. Philipp

Institut für Wärmetechnik und Thermodynamik, Technische Universität Bergakademie Freiberg, Gustav-Zeuner-Str. 7, 09599 Freiberg, Germany

Received 18 January 2005; received in revised form 3 June 2005
Available online 25 October 2005

Abstract

Local reflux condensation heat transfer coefficients have been measured inside a vertical tube with water ($2.6 < Pr_{liq} < 4.5$), ethanol ($12.4 < Pr_{liq} < 18.4$) and isopropanol ($23 < Pr_{liq} < 55$) as the test fluids. A counter current flow situation is established with the liquid film ($0.68 < Re_{film} < 2000$) and the vapour ($1000 < Re_{vap} < 16{,}500$) flowing downward and upward, respectively. The heat transfer has found to be impeded by the shear stress only in cases of a very thin film, i.e. in the smooth laminar range, and it can well be correlated by a simple analytical model. In the laminar-wavy range including developing turbulence the heat transfer coefficients are found to increase with the shear stress, an effect which proved to be enhanced with rising Pr_{liq} numbers. This has been correlated with very good agreement.

Keywords: Heat transfer; Reflux condensation; Falling film; Experiment; Vertical tube; Shear stress effect

1. Introduction

The following situation will be considered here: vapour is flowing upward inside a vertical tube which is cooled from outside leading to condensation at the inner tube walls. In cases of a small enough vapour velocity, a liquid film will form flowing downward counter currently to the vapour—this is what we call reflux condensation. For increasing vapour velocities, however, interactions between the phases bring out critical situations like entrainment of droplets from the film surface, flooding phenomena (starting at the vapour entrance), bridging (with stable liquid columns which are carried over to the exit in long cycle intervals), unstable transition modes (with a climbing film and possible short time oscillations of the liquid column) and finally cocurrent film condensation with both of the phases flowing upward (see, e.g. [1–3]). The tube geometry may vary with respect to diameter, length, inclination angle and shape of the cross-section. Furthermore the vapour may be completely liquified like in a thermosyphon (heat pipe) where the top is closed and the mass flow rates of vapour and liquid are identical. On the other hand, partial condensation leads to a remaining vapour flow at the upper end of the cooling zone.

Much work has been done in the past in the field of condensation heat transfer inside thermosyphons (for an overview see, e.g. [4–7]). Almost all of the publications

* Corresponding author. Tel.: +49 3731 39 2684; fax: +49 3731 39 3655.
E-mail address: gross@iwtt.tu-freiberg.de (U. Gross).

0017-9310/$ - see front matter © 2005 Elsevier Ltd. All rights reserved.
doi:10.1016/j.ijheatmasstransfer.2005.07.030

Nomenclature

c_p	specific heat, kJ/(kg K)
d	tube diameter, m
E	correction factor, dimensionless
g	gravitational acceleration, m/s^2
l	length of condensation zone, m
$\dot{m}$	mass flow rate, kg/s
Nu	Nusselt number, Eq. (1), dimensionless
Pr	Prandtl number, ($\eta c_p/\lambda$), dimensionless
$\dot{q}$	heat flux, W/m^2
Re	Reynolds number, Eq. (2), dimensionless
T	temperature, K
w	velocity, m/s

Greek symbols

α	local heat transfer coefficient, W/(m^2 K)
Δ	difference
δ	film thickness, m
η	dynamic viscosity, Pa s
λ	thermal conductivity, W/(m K)
ν	kinematic viscosity, m^2/s
ξ	friction factor, dimensionless
ρ	density, kg/m^3
τ	shear stress, N/m^2
Ω	factor, dimensionless

Subscripts

corr	correlation
cz	cooling zone
i	inner
liq	liquid
o	outer
red	reduced
ref	reference
TC	thermocouple
vap	vapour
τ	with shear stress
$\tau \to 0$	negligible shear stress

refer to Nusselt's classical solution for the smooth laminar film [8], without any waves at the phase interface and without shear stress effects. Nusselt himself was the first to extend his solution for shear stress effects as the boundary condition in the momentum equation balancing viscous and gravity forces [9]. Later Suematsu et al. [10], Seban and Hodgson [11], Takuma et al. [12], Naidu and Susarla [13], Seban and Faghri [14], Chen et al. [15], Faghri [16], Yang et al. [17] and more recently Pan [18,19] extended the basic model (smooth laminar film) to include vapour flow effects as drag coefficients for laminar and turbulent flow inside tubes with and without closed top, respectively. Some decrease of the local heat transfer coefficients has been found, which is intensified by increasing the vapour velocity , however, this effect keeps negligibly small in most of the cases under consideration. For rising thickness and velocity of the liquid film, disturbances become visible at the up to now smooth film surface where waves are formed playing two roles: (a) the wave crests are sliding down the phase interface with enhanced velocity which brings a reduction of mass flow and film thickness of the remaining parts of the film between the crests; (b) the waves act as turbulence promotors inside the film. Both effects improve condensation heat transfer, increasingly with the Re_{film} number, and they start to play more and more the key role. Takuma et al. [20] showed that these favourable wave effects mostly dominate the negative tailing back due to vapour shear forces. Fukano and Kadoguchi [21] found the local heat transfer coefficients to be strongly increased in high vapour velocity situations, and they attributed this behaviour to enhancement of turbulence inside the liquid film and also to entrainment of droplets. Fiedler et al. [22] primarily investigated inclination effects upon flooding phenomena and, additionally, they found the heat transfer coefficients to exceed Nusselt's no shear solution by some small amount. The thermosphon literature contains lots of experimental investigations, most of which, however, are strongly influenced by non-condensables. In addition to these heat transfer considerations some film thickness measurements can be found. Zhou and Collins [23] applied a rotating needle contact method for film thickness measurements in the smooth laminar range.

Outside the thermosyphon area there are numerous theoretical and experimental investigations in the field of nuclear reactor accident analysis (see, e.g. [24–28]) which are mostly focused on flooding phenomena and respective limits, and only very few of them are dealing with condensation heat transfer. Girard and Chang [29] presented a combined experimental and analytical study of the various reflux condensation phenomena including successful modeling. Chou and Chen [30] and also Park et al. [31] performed some numerical calculations which have been verified with more or less success using thermosyphon experimental data from literature. Finally there is a couple of visual investigations of the two phase interaction in the considered counter current flow situation, e.g., by Karimi and Kawaji [32,33] who applied high speed video photography and a laser-induced photochromic tracer technique in order to investigate liquid motion and the initiation of flooding. An increasingly

interesting new field for reflux condensation with, however, vapour mixtures is found in chemical separation columns where less volatile components are liquified at the wall returning as a liquid film. Respective experimental and analytical work has been done, e.g., by Bartleman et al. [34], and also by Souidi and Bontemps [35].

In all these situations film flow and condensation heat transfer are affected, among others, by shear forces acting between the counter current phases. In earlier experimental investigations the present authors [36–39] have already studied shear-stress effects with water, and correlations from the literature could be confirmed for the limiting case of a stagnant vapour. In the present contribution this investigation is extended to higher liquid *Pr* numbers.

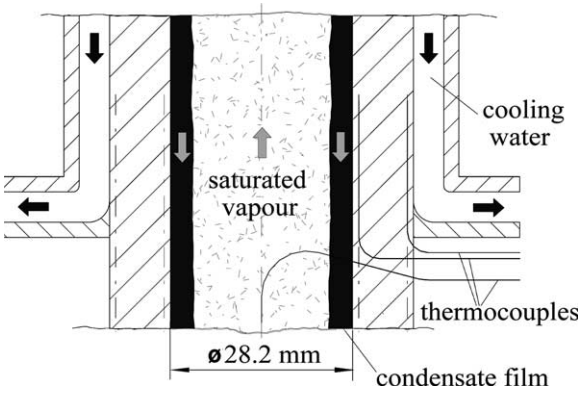

Fig. 2. Measuring arrangement with the thermocouple location.

2. The experiments

2.1. Test rig

For getting reliable experimental data a test rig was planned, designed and constructed (Figs. 1 and 2, for more details see [36,38]) to measure local filmwise condensation heat transfer coefficients in a vertical tube with the total length and inner diameter of 4.2 m and 28.2 mm, respectively. In the limiting case of total condensation, the mass flow rates of vapour and liquid are identical and they can be varied by the simultaneous variation of the heat flow rate supplied to the evaporator and removed again from the condensation zone. Additionally the flow rates of vapour and liquid can be increased independently from each other by two further measures:

- Operation of an external heat exchanger which allows for an extension of the vapour flow rate to the case of non-total condensation. By this, the influence of inert gases is minimized as well.
- Supply of additional liquid at the top of the tube to increase the film flow rate. The respective liquid is fed from the condensate separation device at the tube's lower end, passed through a precooling section (to avoid cavitation), propelled by a speed adjusted gear pump, preheated to saturation state and finally supplied to the upper end of the test tube which is build up from sinter material allowing the liquid to enter the inner tube surface and to form a symmetrically distributed falling liquid film. The water-cooled length of the condensation zone can be varied to obtain a thermal entrance length of either 290, 740 or 1540 mm (denominated as $l_{cz} = 1$, 2 and 3, respectively). The given up liquid returns to the separating device together with the condensate. This completely separate liquid-film cycle allows for an extension of the investigation range for the Re_{film} number and it can be operated with high accuracy.

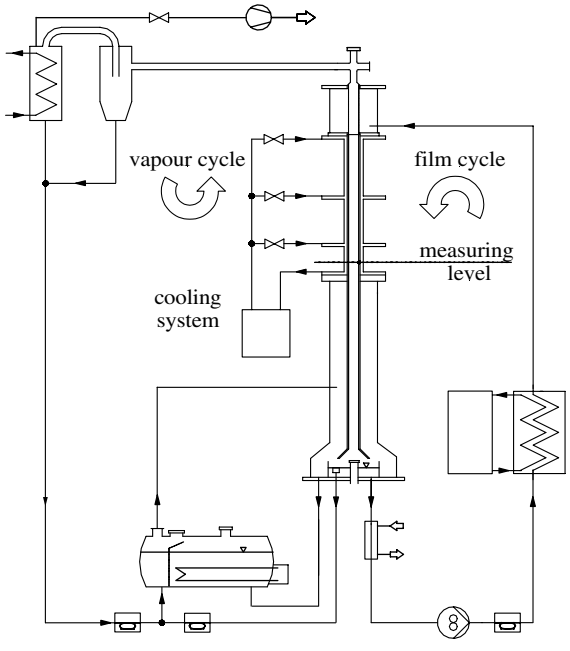

Fig. 1. Schematic drawing of the test facility.

The remaining part of the test tube below the condensation zone serves as an adiabatic vapour flow entrance length (2.2 m).

2.2. Measurements and evaluation

Temperatures, temperature differences, pressures and mass flow rates have been measured at various locations of the vapour and liquid cycles (see [36]). All of these

physical data have been taken with the help of a data acquisition system once per second, and 1-min mean values have been stored during the measuring period of typically 20 min. These 1-min values proved to deviate from each other by less than 1%.

The heat transfer measuring cross-section is located at a level 90 mm above the lower end of the cooling zone (Fig. 1) and it consists of a thickwalled brass tube (Fig. 2). Thermocouples (TC, diameter 0.5 mm) are axially inserted in blind-end bore holes with depth and diameter of 150 and 0.6 mm, respectively, with the remaining gaps filled by tin solder. For recognition of asymmetries a number of independent measuring positions are regularly distributed around the tube with six and three TCs very close to the inner and outer tube surface, respectively. The vapour temperature is measured by one of four thermocouples (diameter 0.25 mm) positioned inside a capillary tube in the center line of the test section. The remaining three ones are connected with respective three inner wall TCs for determination of the temperature difference ΔT_{film} across the film including corrections for the inverse heat conduction close to the inner tube wall surface.

All of the TCs have been calibrated in situ and the same holds for the heat flux which can easily be determined from the measured radial temperature difference ΔT_{wall} inside the wall, the temperature dependent thermal conductivity λ and the radial positions of the thermocouples allowing the determination of heat transfer coefficient and Nu number (Eq. (1)):

$$\dot{q}_{\text{wall,i}} = \frac{2(\lambda\Delta T)_{\text{wall}}}{d_{\text{wall,i}}\ln(d_{\text{TC,o}}/d_{\text{TC,i}})} \quad \alpha = \frac{\dot{q}_{\text{wall,i}}}{\Delta T_{\text{film}}}$$
$$Nu = \frac{\alpha(v_{\text{liq}}^2/g)^{1/3}}{\lambda_{\text{liq}}} \tag{1}$$

The liquid film and vapour Reynolds numbers are evaluated (Eq. (2)) from the respective mass flow rates and viscosities:

$$Re_{\text{film}} = \frac{\dot{m}_{\text{liq}}}{\pi d_{\text{wall,i}}\eta_{\text{liq}}} \quad Re_{\text{vap}} = \frac{4\dot{m}_{\text{vap}}}{\pi d_{\text{film,i}}\eta_{\text{vap}}}$$
$$\text{with } d_{\text{film,i}} \approx d_{\text{wall,i}} \tag{2}$$

The detailed analysis of the various influences brought ±3.5% and ±0.3% for the overall uncertainties of the evaluated Nu and Re numbers, respectively [36]. The shear stress is derived from pressure loss measurements in the lower part of the tube and generally it agrees rather good with correlations from literature. The same holds for pressure loss results derived from saturation-temperature profiles measured in the vapour phase along the tube. Despite this, the uncertainties of both of these measurements, however, proved to be unacceptable large and so the shear stress at the vapour–liquid interface

$$\tau = E\frac{\xi}{8}\rho_{\text{vap}}w_{\text{vap}}^2 \quad \text{and}$$
$$\tau^* = \frac{\tau}{g(\rho_{\text{liq}}-\rho_{\text{vap}})(v_{\text{liq}}^2/g)^{1/3}}\,(\text{dimensionless}) \tag{3}$$

has finally been calculated from friction factors following Eqs. (4)–(7) [40,41] where E is a correction factor for condensation

$$\xi = \frac{358}{\Omega^2} + \frac{0.205}{\Omega^{0.25}} \quad \text{with}$$
$$\Omega = c\frac{Re_{\text{vap}}}{Re_{\text{film}}^n}\left(\frac{\rho_{\text{liq}}}{\rho_{\text{vap}}}\right)^{2/5}\left(\frac{\eta_{\text{vap}}}{\eta_{\text{liq}}}\right)^{2/3}\left(\frac{2\delta_{\tau\to 0}}{d_{\text{wall,i}}}\right)^{1/2} \tag{4}$$

with the parameters

$$\left.\begin{matrix} c = 1.31 \\ n = 0.25 \end{matrix}\right\} \quad \text{for } Re_{\text{film}} < 40$$

and

$$\left.\begin{matrix} c = 4.76 \\ n = 0.6 \end{matrix}\right\} \quad \text{for } Re_{\text{film}} \geqslant 40 \tag{5}$$

and the film thickness for negligible shear stress

$$\delta_{\tau\to 0} = (3Re_{\text{film}})^{1/3}(v_{\text{liq}}^2/g)^{1/3} \quad \text{for } Re_{\text{film}} < 516 \tag{6}$$

and

$$\delta_{\tau\to 0} = 0.303Re_{\text{film}}^{0.583}(v_{\text{liq}}^2/g)^{1/3} \quad \text{for } Re_{\text{film}} \geqslant 516 \tag{7}$$

All the properties are taken at a mean temperature inside the liquid film $T_{\text{ref}} = T_{\text{wall,i}} + f_{\text{ref}}\Delta T_{\text{film}}$ with $f_{\text{ref}} = 0.25$ for the viscosity and $f_{\text{ref}} = 0.5$ for all other.

2.3. Experimental procedure

The measurements have been taken in steady-state conditions with the main parameters as given in Table 1:

- The Pr_{liq} number is varied by changing the test fluid and to a smaller extent by temperature variations.
- The smallest Re_{film} numbers are established by operating only the short lower cooling circuit ($l_{\text{cz}} = 1$). In a first step Re_{film} can be increased by a decrease of the cooling water temperature (keeping the vapour temperature constant). Changing to the intermediate and the long cooling water cycle ($l_{\text{cz}} = 2$ and 3, respectively) yields a stepwise increase of Re_{film} which can further be raised by the supplement of liquid at the top of the tube.
- The Re_{vap} number, and in the same step the dimensionless shear stress τ^*, can again be varied by a combination of measures. The smallest shear stress is obtained with the shortest condensation length and the smallest heat flux which, however, has been kept

Table 1
Main parameters of the experiments

	Pr_{liq}	Re_{film}	Re_{vap}
Water	2.6–4.5	1.5–2100	1000–15,000
Ethanol	12.4–18.4	3.5–220	1600–16,500
Isopropanol	23–55	0.68–180	3500–15,000

regularly above 10^4 W/m^2 in the present experiments, corresponding to approximately $\Delta T_{wall} = 1$ K. The shear stress has mainly been raised by increasing (a) the length of the cooling zone and (b) the cooling power of the external condenser until the flooding limit is achieved.

3. Results and discussion

The complete set of measured data includes quite a lot of data points which are characterized by identical main parameters (Re_{film}, Pr_{liq}, τ^*) but measured with different values of the cooling zone length (l_{cz}). The agreement of such data has been checked, and it was found that there is some entrance-length effect on heat transfer for turbulent film flow. In the next section only those data with $l_{cz} = 2$ and 3 (with some exceptions) have been considered. The entrance-length effect will be subject of further investigations.

Shear stress has been found to reduce the heat transfer coefficients in cases of an extremely thin (smooth laminar) film. This will be discussed in a first step. With increasing the film thickness, i.e. the Re_{film} number, an intensification of heat transfer with a rising shear stress has been observed. This holds for the laminar-wavy film including the regime of developing turbulence.

3.1. Smooth laminar range ($Re_{film,water} < 7$ and $Re_{film,isopropanol} < 3$)

Results are presented for the smallest and highest Pr_{liq} numbers in Figs. 3 and 4, respectively, where Nu is plotted vs. the dimensionless shear stress for various Re_{liq} numbers interconnected by respective thin trend lines.

With water ($2.6 \leqslant Pr_{liq} \leqslant 4.5$, Fig. 3) and also with isopropanol ($28 \leqslant Pr_{liq} \leqslant 52$, Fig. 4), the shear stress is found to bring different effects on heat transfer primarily depending on Re_{film}. In the nearly wave free laminar range (i.e. for $Re_{film,water} < 6, \ldots, 7$ and $Re_{film,isopropanol} < 3$, approximately corresponding to $Re_{film} = 0.47Ka^{-0.1}$ as the accepted lower limit for wave formation [42]) the Nu number is found to decrease with rising the shear stress, an effect which becomes less pronounced when Re_{film}, i.e. thickness and velocity of the liquid film, increase. The characteristic starts to change around $Re_{film} = 10$ (water) and $Re_{film} = 4$ (isopropanol),

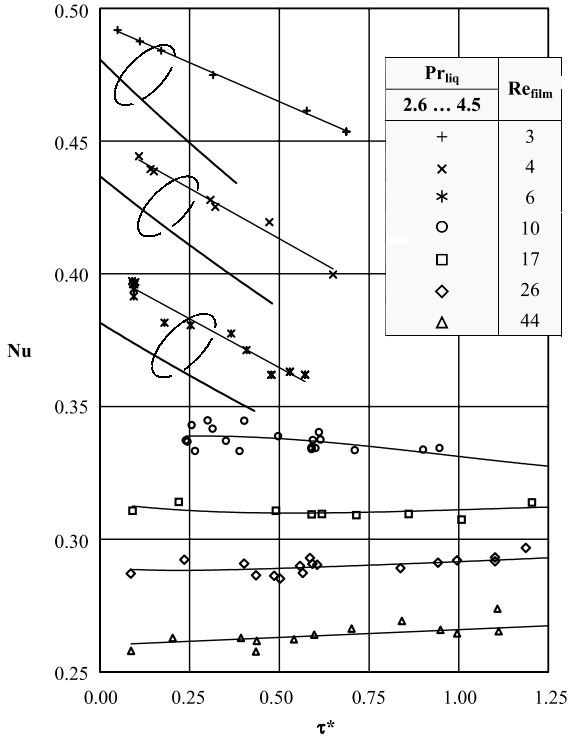

Fig. 3. Shear stress effect on heat transfer for water in the low Re_{film} range with the bold lines representing Eq. (11).

respectively, and transition is found to a more-or-less slight increase of Nu with the shear stress. For a certain Re_{film} number (e.g., $Re_{film} \approx 6$), the onset of transition clearly depends on Pr_{liq}. A strong increase of Nu with τ^* is found for $Pr_{liq} = 52$ (◇, Fig. 4) whereas the transition is delayed for $Pr_{liq} = 28$ (♦, Fig. 4) and finally for $Pr_{liq} = 3.6$ (∗, Fig. 3) it is not discernible at all. The film flow is obstructed by the counter current vapour flow and the associated shear stress. The film thickness is being increased by this and the heat transfer shows a tendency to decrease. This effect is clearly visible in the lowest Re_{film} range where Nusselt's theory applies.

The assumption of pure conduction through the film brings

$$\alpha = \frac{\lambda_{liq}}{\delta_{film}} \quad \text{and}$$

$$Nu = \frac{\alpha(\nu_{liq}^2/g)^{1/3}}{\lambda_{liq}} = \frac{1}{\delta_{film}^+} \quad \text{with } \delta_{film}^+ = \frac{\delta_{film}}{(\nu_{liq}^2/g)^{1/3}} \tag{8}$$

with δ_{film} as the film thickness which is obtained from a simple balance of viscose and gravity forces. The no-shear boundary condition at the vapour side [8] has to be replaced by a respective shear force [9] for non-zero vapour velocity yielding

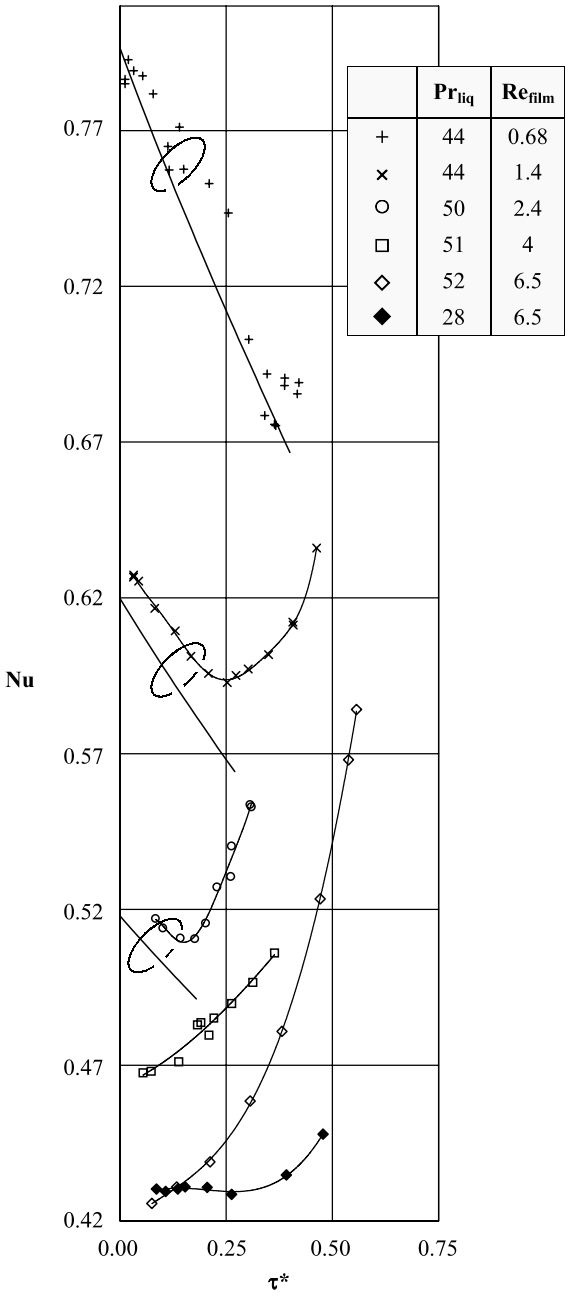

Fig. 4. Shear stress effect on heat transfer for isopropanol in the low Re_{film} range with the bold lines representing Eq. (11).

$$Re_{\text{film}} = \frac{\delta_{\text{film}}^{+3}}{3} - \frac{\delta_{\text{film}}^{+2}}{2}\tau^* \tag{9}$$

With an approximation by Thumm [36] the following Eqs. (10) and (11) for the combined effects of Re_{film} number and τ^* upon dimensionless film thickness and Nu number are obtained as

$$\delta_{\text{film}}^{+} = 0.59\tau^* + (3^{1/3} - 0.0086\tau^*)(Re_{\text{film}} + 0.28\tau^{*3})^{1/3} \tag{10}$$

$$Nu = \left[0.59\tau^* + (3^{1/3} - 0.0086\tau^*)(Re_{\text{film}} + 0.28\tau^{*3})^{1/3}\right]^{-1} \tag{11}$$

The deviation between Eq. (10) and the numerical solution of Eq. (9) is very small and keeps below 1% in the total range of the present investigations ($0 < \tau^* < 3$ and $Re_{\text{film}} > 0.5$).

Eq. (11) has been evaluated for selected parameters and the results are plotted in Figs. 3 and 4 as bold lines together with the respective experimental findings. A clear confirmation of the trends is yielded with good agreement for cases with very low Re_{film}. The present experiments show that this simple model which can be found in many publications is only valid for selected cases with an extremely thin film. The deviations from the experimental results rapidly increase with rising film thickness (Re_{film}) and shear stress τ^*. In this case a second effect obviously becomes active.

3.2. Intermediate Re_{film} numbers (laminar-wavy and turbulent film)

Fig. 5 brings series of data points for selected classes of the Pr_{liq} number. The water data (Fig. 5a and b) show an extension of the characteristic indicated in Fig. 3 for a wide range of $Re_{\text{film}} > 27$ with a slight increase of Nu with τ^*. With ethanol, the Prandtl number as the viscosity to diffusivity ratio is raised by a factor of 4 or 5. This means that damping of velocity fluctuations will be much stronger when compared with temperature fluctuations. Fig. 5c and d shows the results of the ethanol experiments for two different Pr_{liq} values and the shear stress effects are found to be stronger that in the water cases. The same findings hold for further increased Pr_{liq} numbers with isopropanol (see Fig. 5e and f) where the shear stress effect obviously is further enhanced.

Now the conjugated shear stress and Pr_{liq} effects on condensation heat transfer will be correlated. As a first step the variation of Nu with τ^* in Fig. 5a–f has been analyzed, and the relative increase of the Nu number is found to be

$$\frac{Nu - Nu_{\tau\to 0}}{Nu_{\tau\to 0}} \propto 0.18\tau^* + \tau^{*2.2} \tag{12}$$

independently of Re_{film}. There is, however, a strong Pr_{liq} influence upon the intensity of the shear stress effect (Fig. 5):

$$Nu_{\text{red}} = \frac{Nu - Nu_{\tau\to 0}}{Nu_{\tau\to 0}(0.18\tau^* + \tau^{*2.2})} = f(Pr_{\text{liq}}) \tag{13}$$

This can clearly be seen in Fig. 6 where Nu_{red} is plotted vs. Pr_{liq}, and the effect can well be correlated by Eq. (14):

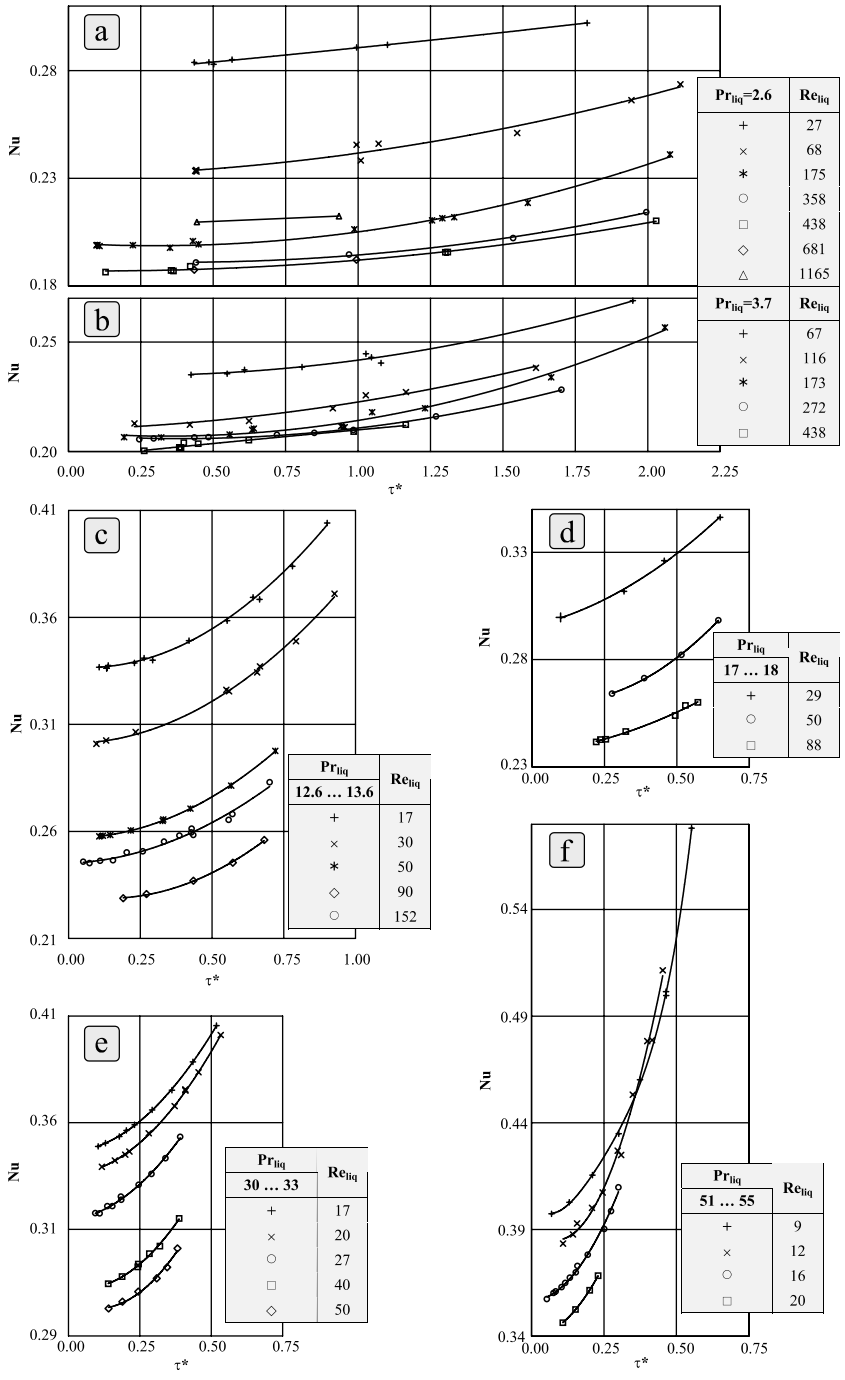

Fig. 5. Shear stress effect on heat transfer in the laminar-wavy and turbulent range: (a,b) for water, (c,d) for ethanol, (e,f) for isopropanol.

$$Nu_{\mathrm{red}} = -0.025 + 0.016 Pr_{\mathrm{liq}}^{1.08} \tag{14}$$

$$Nu_{\mathrm{corr}} = Nu_{\tau\to 0}[1 + (0.18\tau^{*} + \tau^{*2.2})(-0.025 + 0.016 Pr_{\mathrm{liq}}^{1.08})] \tag{15}$$

Combining Eqs. (13) and (14) brings the following correlation for the conjugated effects:

valid for the laminar-wavy range including transition to turbulence (see Fig. 5).

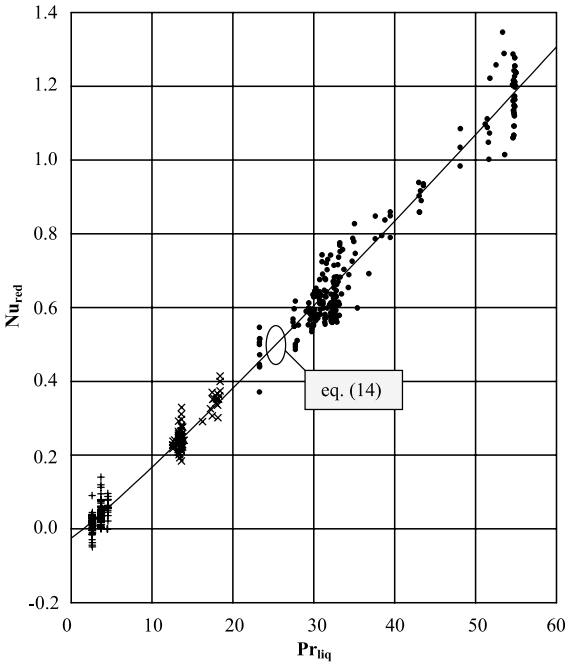

Fig. 6. Pr_{liq} number effect on the intensification of heat transfer.

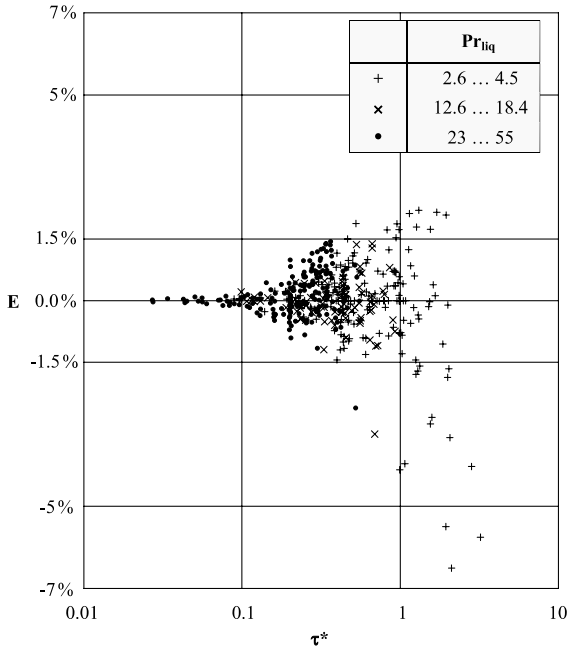

Fig. 8. Correlation error as a function of τ^*.

Figs. 7 and 8 show the relative deviations E between Eq. (15) and the measured data as a function of film Reynolds number and dimensionless shear stress, respectively. It is clearly shown that almost all of the measured results (448 out of 486, i.e. 94%) can be correlated within ±1.5% with the exception of some of the water results at extremely high shear stress (mostly $\tau^* > 1$) where the begin of transition to flooding has to be argued.

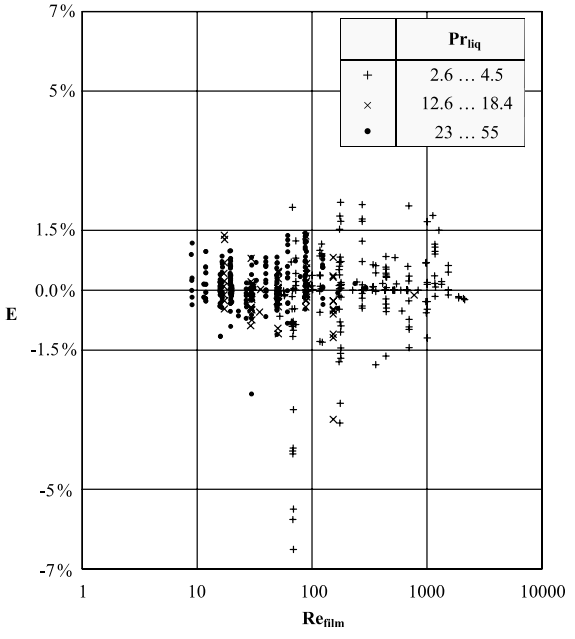

Fig. 7. Correlation error as a function of Re_{film} number.

3.3. Heat transfer close to the flooding limit

Close to the flooding limit the liquid film flow changes its characteristic into a pulsating one with intermittently accumulation and upward ejection of liquid. With water as the test fluid, flooding occurs suddenly and without any warning sign. With ethanol and in particular with isopropanol transition to flooding is escorted by a gradual liquid discharge. Special features of film flow and heat transfer have been observed. Due to the geometrical situation (inside a that narrow tube) the film flow could not be visually observed in detail. However, the wall temperatures in the measuring section were taken at three positions shifted by 120°, and unequal heat transfer distributions at the scope can be observed (normally these temperatures agree within narrow limits). When approaching the flooding limit, the heat transfer coefficients increase disproportionally strong, and big differences are found at the scope.

4. Evaluation for the limiting case of zero shear stress

Additionally the experimental results (Fig. 5a–f) have been evaluated for the limiting case of zero shear stress

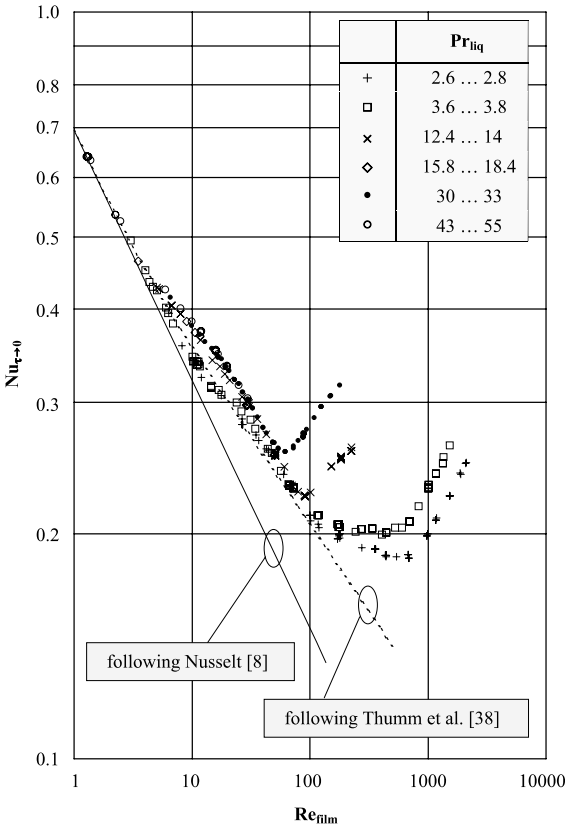

Fig. 9. Non-shear stress Nu number vs. Re_{film} number.

by extrapolation following Eq. (15). Respective data are plotted in Fig. 9 as Nu vs. Re_{film} numbers where the typical ranges of smooth laminar film (following Nusselt's theory), the laminar-wavy range and the transition to turbulence can clearly be seen. Evaluated local Nu numbers perfectly follow Nusselt's theory for about $Re_{film} < 3$. Beyond this limit the well known enhancement due to wave formation is obtained which can be described by a wave factor as given, e.g., by Thumm et al. [38] as indicated in Fig. 9. This behaviour is true for water whereas ethanol and isopropanol with the much higher Pr_{liq} shows some additional increase. Transition to turbulence is found in the expected way with a smooth characteristic for water and a more abrupt increase of Nu numbers in case of the higher Pr_{liq} numbers. The parameter ranges of film and vapour Re numbers were limited in the present investigations due to the counter flow situation and the occurrence of the flooding limit.

5. Conclusions

Local condensation heat transfer coefficients have been measured in a vertical tube for countercurrent flow of vapour and liquid with water, ethanol and isopropanol in wide ranges of Prandtl and Reynolds numbers. The influence of shear stress on the Nusselt number depends obviously on the kind of film flow. For small film Reynolds numbers the shear stress restrains the film flow and Nusselt numbers decrease, for larger Reynolds numbers wave formation, local turbulence and thus the mixing of the film are enhanced which leads to an increase of the Nusselt number. There is a transition range with compensation of these two effects. With rising liquid Prandtl numbers the effect of heat transfer enhancement becomes stronger which has been correlated with Pr_{liq} and the dimensionless shear stress τ^*. There are additional effects due to the film entrance length which have to be further investigated.

Acknowledgements

The support of this work by the Deutsche Forschungsgemeinschaft (DFG) is greatly appreciated. Furthermore the authors like to thank Andreas Wahl and also their former colleague Sven Thumm for their contributions.

References

[1] I.F. Obinello, G.F. Round, J.S. Chang, Condensation enhancement by steam pulsation in a reflux condenser, Int. J. Heat Fluid Flow 15 (1) (1994) 20–29.
[2] A. Zapke, D.G. Kröger, Countercurrent gas–liquid flow in inclined and vertical ducts—I: Flow patterns, pressure drop characteristics and flooding, Int. J. Multiphase Flow 26 (2000) 1439–1455.
[3] J. Palen, Z.H. Yang, Reflux condensation flooding prediction: review of current status, Trans. IchemE 79 (Part A) (2001) 463–469.
[4] U. Gross, E. Hahne, Reflux condensation inside a two-phase thermosyphon at pressures up to the critical, in: Proc. 8th Int. Heat Transfer Conf., vol. 4, San Francisco 1986, pp. 1613–1620.
[5] U. Gross, E. Hahne, Condensation heat transfer inside a closed thermosyphon—generalized correlation of experimental data, in: Proc. 6th Int. Heat Pipe Conf., vol. 3, Grenoble, 1987, pp. 466–471.
[6] U. Gross, Kondensation und Verdampfung im geschlossenen Thermosyphon, Fortschrittsbericht VDI, Reihe 19, No. 46, VDI Verlag, Düsseldorf, 1991.
[7] U. Gross, Reflux condensation heat transfer inside a closed thermosyphon, Int. J. Heat Mass Transfer 35 (1992) 279–294.
[8] W. Nusselt, Die Oberflächenkondensation des Wasserdampfs, Z. Ver. Dt. Ing. 60 (1916) 541–569.
[9] W. Nusselt, Die Oberflächenkondensation des Wasserdampfs, Z. Ver. Dt. Ing. 60 (1916) 569–575.
[10] H. Suematsu, K. Harada, S. Inoue, J. Fujita, Y. Wakiyama, Heat transfer characteristics of heat pipes, Heat Transfer-Jpn. Res. 7 (1) (1978) 1–22.

[11] R.A. Seban, J.A. Hodgson, Laminar film condensation in a tube with upward vapor flow, Int. J. Heat Mass Transfer 25 (1982) 1291–1300.
[12] M. Takuma, S. Maezawa, A. Tsuchida, Studies on condensation heat transfer in two-phase closed thermosyphons, Inst. Space Astron. Sci. Rep. 1 (1983) 247–255.
[13] B.R. Naidu, S. Susarla, Comment on 'laminar film condensation in a tube with upward vapour flow' by Seban and Hodgson, Int. Commun. Heat Mass Transfer 10 (1983) 445–449.
[14] R.A. Seban, A. Faghri, Film condensation in a vertical tube with a closed top, Int. J. Heat Mass Transfer 27 (1984) 944–948.
[15] S.J. Chen, J.G. Reed, C.L. Tien, Reflux condensation in a two-phase closed thermosyphon, Int. J. Heat Mass Transfer 27 (1984) 1587–1594.
[16] A. Faghri, Turbulent film condensation in a tube with concurrent and countercurrent vapor flow, AIAA Paper, AIAA-86-1354, AIAA/ASME in: 4th Joint Thermophys. and Heat Transfer Conf., Boston, 1986.
[17] L. Yang, T. Chen, J. Xu, Effects of interphase shear on reflux condensation heat transfer flowing in vertical circular tube, Hedongli Gongcheng/Nucl. Power Eng. 16 (2) (1995) 154–160 (in Chinese).
[18] Y. Pan, Condensation heat transfer characteristics and concept of sub-flooding limit in a two phase closed thermosyphon, Int. Commun. Heat Mass Transfer 28 (2001) 311–322.
[19] Y. Pan, Condensation characterisics inside a vertical tube considering the presence of mass transfer, vapor velocity and interfacial shear, Int. J. Heat Mass Transfer 44 (2001) 4475–4482.
[20] M. Takuma, S. Maezawa, A. Tsuchida, Condensation heat transfer characteristics of the annular two-phase closed thermosyphon, Nippon Kikai Gakkai Ronbunshu, B-hen 52 (482) (1986) 3537–3544.
[21] T. Fukano, Local heat transfer in reflux condensation inside aclosed two-phase thermosyphon, in: Proc. 9th Int. Heat Transfer Conf., vol. 3, Jerusalem, 1990, pp. 85–90.
[22] S. Fiedler, H. Auracher, Experimental and theoretical investigation of reflux condensation in an inclined small diameter tube, Int. J. Heat Mass Transfer 47 (2004) 4031–4043.
[23] X. Zhou, R.E. Collins, Condensation in a gas-loaded thermosphon, Int. J. Heat Mass Transfer 38 (1995) 1605–1617.
[24] Y.J. Hae, N.K. Bum, L. Kwangho, Thermal-hydraulic phenomena during reflux condensation cooling in steam generator tubes, Ann. Nucl. Energy 25 (17) (1998) 1419–1428.
[25] T.J. Liu, Reflux condensation behaviour in a U-tube steam generator with or without noncondensables, Nucl. Eng. Des. 204 (1–3) (2001) 221–232.
[26] H.Y. Jeong, Prediction of counter-current flow limitation at hot leg pipe during a small-break LOCA, Ann. Nucl. Energy 29 (5) (2002) 571–583.
[27] K. Umminger, R. Mandl, R. Wegner, Restart of natural circulation in a PWR-PKL: test results and S-RELAP5 calculations, Nucl. Eng. Des. 215 (1–2) (2002) 39–50.
[28] S.K. Mousavian, F. d'Auria, M.A. Salehi, Analysis of natural circulation phenomena in VVER-1000, Nucl. Eng. Des. 229 (2004) 25–46.
[29] R. Girard, J.S. Chang, Reflux condensation phenomena in single vertical tubes, Int. J. Heat Mass Transfer 35 (1992) 2203–2218.
[30] G.H. Chou, J.C. Chen, A general modeling for heat transfer during reflux condensation inside vertical tubes surrounded by isothermal fluid, Int. J. Heat Mass Transfer 42 (1999) 2299–2311.
[31] H.S. Park, H.C. No, Y.S. Bang, Analysis of experiments for in-tube steam condensation in the presence of noncondensable gases at a low pressure using the RELAP5/MOD3.2 code modified with a con-iterative condensation model, Nucl. Eng. Des. 225 (2003) 173–190.
[32] G. Karimi, M. Kawaji, Flow characteristics and circulatory motion in wavy falling films with and without countercurrent gas flow, Int. J. Multiphase Flow 25 (1999) 1305–1319.
[33] G. Karimi, M. Kawaji, Flooding in vertical countercurrent annular flow, Nucl. Eng. Des. 200 (2000) 95–105.
[34] A. Bartleman, D. Cuthbertson, C.D. Grant, J.M. McNaught, Some results for reflux condensation of hydrocarbon vapour mixtures, Trans. IChemE 80 (Part A) (2002) 295–300.
[35] N. Souidi, A. Bontemps, Reflux condensation in narrow rectangular channels with perforated fins, Appl. Thermal Eng. 23 (2003) 871–891.
[36] S. Thumm, Filmkondensation im senkrechten Rohr bei Gegenstrom von Dampf und Flüssigkeit, PhD Thesis, Technische Universität Bergakademie Freiberg, Freiberg, Germany, 2000.
[37] S. Thumm, Ch. Philipp, U. Gross, Experimental investigation of the influence of countercurrent flow of the phases on condensation heat transfer in a vertical tube, in: E.W.P. Hahne, W. Heidemann, K. Spindler (Ed.), Proc. of 3rd Eur. Thermal Sci. Conf. 2000, Heidelberg, Germany, ETS, Pisa, 2000, pp. 933–938.
[38] S. Thumm, Ch. Philipp, U. Gross, Film condensation of water in a vertical tube with countercurrent vapour flow, Int. J. Heat Mass Transfer 44 (2001) 4245–4256.
[39] U. Gross, Ch. Philipp, S. Thumm, Effect of countercurrent vapour flow on film condensation heat transfer inside a vertical tube, Heat Transfer 2002, in: Proc. 12th Int. Heat Transfer Conf., Grenoble, pp. 923–928.
[40] H. Brauer, Grundlagen der Einphasen-und Mehrphasenströmungen, Sauerländer Verlag, Aarau and Frankfurt, 1971.
[41] F. Blangetti, R. Krebs, Filmkondensation reiner Dämpfe, in: VDI-Wärmeatlas, VDI Verlag, Düsseldorf, 1994.
[42] S.V. Alekseenko, V.E. Nakoryakov, B.G. Pokusaev, Wave Formation of Liquid Films, Begell House, New York, 1994.